AIP | APL Materials

NOW INDEXED IN THOMSON REUTERS DATABASES

Morphology-photovoltaic property correlation in perovskite solar cells: One-step versus two-step deposition of CH3NH3PbI3

Jeong-Hyeok Im, Hui-Seon Kim, and Nam-Gyu Park

Citation: APL Materials **2**, 081510 (2014); doi: 10.1063/1.4891275
View online: http://dx.doi.org/10.1063/1.4891275
View Table of Contents: http://scitation.aip.org/content/aip/journal/aplmater/2/8?ver=pdfcov
Published by the AIP Publishing

APL MATERIALS **2**, 081510 (2014)

Morphology-photovoltaic property correlation in perovskite solar cells: One-step versus two-step deposition of $CH_3NH_3PbI_3$

Jeong-Hyeok Im, Hui-Seon Kim, and Nam-Gyu Park[a]
School of Chemical Engineering and Department of Energy Science, Sungkyunkwan University, Suwon 440-746, South Korea

(Received 21 April 2014; accepted 14 July 2014; published online 28 July 2014)

Perovskite $CH_3NH_3PbI_3$ light absorber is deposited on the mesoporous TiO_2 layer via one-step and two-step coating methods and their photovoltaic performances are compared. One-step coating using a solution containing CH_3NH_3I and PbI_2 shows average power conversion efficiency (PCE) of 7.5%, while higher average PCE of 13.9% is obtained from two-step coating method, mainly due to higher voltage and fill factor. The coverage, pore-filling, and morphology of the deposited perovskite are found to be critical in photovoltaic performance of the mesoporous TiO_2 based perovskite solar cells. [http://dx.doi.org/10.1063/1.4891275]

Perovskite solar cell is emerging photovoltaic technology because of low cost and high efficiency. Since the reports on the all-solid-state perovskite solar cells with power conversion efficiencies (PCEs) of ~10% in 2012,[1,2] rapid progress has been made for the past one and half years. As a consequence, PCEs as high as over 16% have been achieved.[3,4] $CH_3NH_3PbI_3$ and $CH_3NH_3PbI_{3-x}Cl_x$ are currently the front-and-center materials for high efficiency perovskite solar cell. Since perovskite was first used as a sensitizer in dye-sensitized type solar cell in the early stage,[5,6] perovskite has been tried to be deposited on the surface of TiO_2. Spin-coating of the solutions containing CH_3NH_3I and PbI_2 for $CH_3NH_3PbI_3$ or CH_3NH_3I and $PbCl_2$ for $CH_3NH_3PbI_{3-x}Cl_x$ led to the scattered nanodots[1] or extremely thin layer.[2] This method requires infiltration of hole transporting material (HTM), such as 2,2′,7,7′-tetrakis(*N*,*N*-di-*p*-methoxyphenylamine)-9,9-spirobifluorene (spiro-MeOTAD), into the pores of the metal oxide films. Photovoltaic performance relies significantly on the extent of pore-filling with HTM. This issue was addressed by filling the pores with perovskite instead of HTM,[7] which resulted in a PCE of 12%. Building up the perovskite thin layer in the mesoporous metal oxide matrix (nanocomposite structure) eventually led to construction of heterojunction structure without the metal oxide layer.[4] Recent progress in perovskite solar cell and its basic understanding can be found in the latest literatures.[8–12]

For pore-filling with $CH_3NH_3PbI_3$ perovskite, sequential deposition technique via two-step dipping was found to one of effective ways to achieve reproducibly high efficiency perovskite solar cell.[3] Average PCE of 12% with small standard deviation of ±0.5 was obtained using two-step dipping method. A slight modification of dipping condition led to a PCE of 15%. It was mentioned that uncontrolled precipitation of $CH_3NH_3PbI_3$ perovskite in a single step deposition produced large morphological variation and thereby inconsistent photovoltaic performance. However, no comparative study between the one-step and two-step deposition has been carried out. Here we have studied morphology and photovoltaic performance depending on deposition procedure of $CH_3NH_3PbI_3$. We performed two-step sequential spin-coating procedure for $CH_3NH_3PbI_3$ deposition which was slightly different from two-step dipping method.[3] Both one-step and two-step coating methods

[a]Author to whom correspondence should be addressed. Electronic mail: npark@skku.edu. Tel.: +82-31-290-7241. Fax: +82-31-290-7272.

resulted in reproducible photovoltaic performance, but significant difference in especially photovoltage and fill factor. Electron life time was dependent on coating procedure. Such difference in photovoltaic performance was found to correlate to morphology of the deposited $CH_3NH_3PbI_3$.

CH_3NH_3I was synthesized according to method reported in Ref. 6. Methylamine (27.86 ml, 40% in methanol, TCI) and hydroiodic acid (30 ml, 57 wt.% in water, Aldrich) were mixed at 0 °C and stirred for 2 h. The precipitate was recovered by evaporation at 50 °C for 1 h. The product was washed with diethyl ether three times and then finally dried at 60 °C in vacuum oven for 24 h.

Anatase TiO_2 nanoparticles with diameter of ~40 nm were synthesized by two-step hydrothermal method. The seed particles with diameter of ~20 nm were synthesized by acetic acid catalyzed hydrolysis of titanium isopropoxide (97%, Aldrich) and autoclaving at 230 °C for 12 h. The seed particles were washed with ethanol and collected using centrifuge. Hydrothermal treatment was performed again with the seed particles to grow the particle size. TiO_2 paste was prepared by mixing the TiO_2 particles (~40 nm) with terpineol (99.5%, Aldrich), ethyl cellulose (EC) (46 cp, Aldrich), and lauric acid (LA) (96%, Fluka) at nominal ratio of TiO_2:TP:EC:LA = 1.25:6:0.6:0.1. The paste was further treated with three-roll-mill for 40 min.

FTO (Fluorine-doped Tin Oxide) glass substrate (Pilkington, TEC-8, 8 Ω/sq) with dimension of 2.5 cm × 2.5 cm was cleaned in an ultrasonic bath containing ethanol for 20 min, which was treated in UVO (Ultraviolet Ozone) cleaner for 20 min. TiO_2 blocking layer (BL) was spin-coated on a FTO substrate at 2000 rpm for 20 s using 0.15M titanium diisopropoxide bis(acetylacetonate) (75 wt.% in isopropanol, Aldrich) in 1-butanol (99.8%, Aldrich) solution, which was heated at 125 °C for 5 min. After cooling down to room temperature, the TiO_2 paste was spin-coated on the BL layer at 2000 rpm for 10 s, where the pristine paste was diluted in ethanol (0.1 g/ml). After drying at 100 °C for 5 min, the film was annealed at 550 °C for 30 min. The mesoporous TiO_2 film was immersed in 0.02M aqueous $TiCl_4$ (>98%, Aldrich) solution at 90 °C for 10 min. After washing with de-ionized (DI) water and drying, the film was heated at 500 °C for 30 min.

To make the perovskite precursor solution, the synthesized CH_3NH_3I (0.395 g) was mixed with PbI_2 (1.157 g, 99% Aldrich) in 2 ml *N*,*N*-dimethylacetamide (DMA, >99% Sigma) at 60 °C for 12 h under stirring. Twenty microliters perovskite precursor solution was spin-coated on the mesoporous TiO_2 layer at 3000 rpm for 20 s. The film was dried consecutively at 40 °C for 3 min and 100 °C for 5 min. Twenty microliters of spiro-MeOTAD solution was spin-coated on the $CH_3NH_3PbI_3$ perovskite layer at 4000 rpm for 30 s. A spiro-MeOTAD solution was prepared by dissolving 72.3 mg of spiro-MeOTAD in 1 ml of chlorobenzene, to which 28.8 μl of 4-*tert*-butyl pyridine (TBP) and 17.5 μl of lithium bis(trifluoromethanesulfonyl)imide (Li-TFSI) solution (520 mg Li-TSFI in 1 ml acetonitrile (Sigma-Aldrich, 99.8%)) were added. Finally, an 80-nm-thick gold electrode was thermally deposited on the spiro-MeOTAD coated film. The one substrate contains five cells and the photoactive layer of each cell was ca. 0.2 cm^2 (Figure S1 of the supplementary material).[13]

In 1 ml *N*,*N*-dimethylformamide (DMF, 99.8% Sigma-Aldrich), 462 mg PbI_2 was dissolved at 70 °C to make 1M PbI_2 solution. Twenty microliters PbI_2 solution was spin-coated on the mesoporous TiO_2 layer at 3000 rpm for 20 s, which was dried at 40 °C for 3 min and 100 °C for 5 min consecutively. One hundred microliters of 0.063M CH_3NH_3I solution in 2-propanol (Aldrich) (10 mg/ml) was loaded on the PbI_2-coated substrate for 20 s, which was spun at 4000 rpm for 20 s and then dried at 100 °C for 5 min. It took 4 s to reach 4000 rpm, the duration for acceleration. The HTM and Au layer were formed by the same way in the one-step coating procedure.

Photocurrent and voltage were measured from a solar simulator equipped with 450 W Xenon lamp (Newport 6279 NS) and a Keithley 2400 source meter. Light intensity was adjusted with the NREL-calibrated Si solar cell having KG-2 filter for approximating one sun light intensity (100 mW cm^{-2}). While measuring current and voltage, the cell was covered with a black mask having an aperture. Incident photon-to-electron conversion efficiency (IPCE) was measured using a specially designed IPCE system (PV measurement, Inc.). A 75 W Xenon lamp was used as a light source for generating monochromatic beam. Calibration was accomplished using a silicon photodiode, which was calibrated using the NIST-calibrated photodiode G425 as a standard. IPCE data were collected at DC mode. A field-emission scanning electron microscope (FE-SEM, Jeol JSM 6700F) was used to investigate surface and cross sectional morphology of the perovskite solar cells.

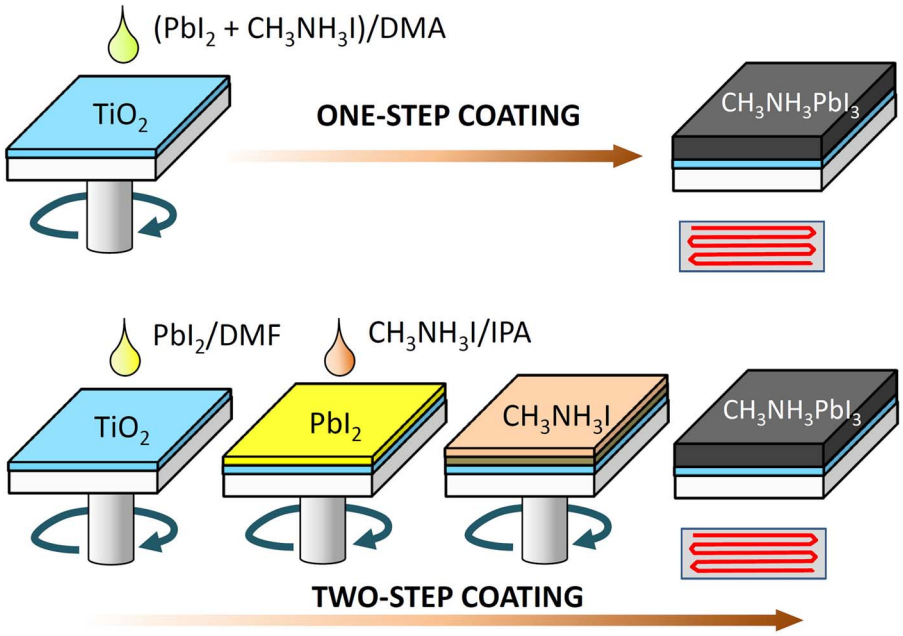

FIG. 1. One-step and two-step spin-coating procedures for $CH_3NH_3PbI_3$ formation. PbI_2 was mixed with CH_3NH_3I in *N*,*N*-dimethylacetamide (DMA), which was spin-coated and heated for one-step coating. For two-step coating, a PbI_2-dissolved *N*,*N*-dimethylformamide (DMF) solution was first spin-coated on the substrate, dried and then a CH_3NH_3I-dissolved isopropyl alcohol (IPA) solution was spin-coated on the PbI_2 coated substrate.

For transient photovoltage measurement, 535 nm and 680 nm of wavelength lasers were used as probe and bias light source, respectively. The probe light was incident over the bias light generating steady-state charge where the incident charge was rapidly decreased showing first order exponential decay. Both light intensities were varied by a neutral density filter. The transient photovoltage signal was amplified using a low-noise preamplifier, Stanford Research System SR560 and monitored by an oscilloscope, TDS 3054B. Impedance spectra were measured in dark with an Autolab 302 B with varying a bias potential from 0 V to 1.0 V where the potential step is 0.1 V. AC 20 mV perturbation was applied with a frequency from 1 MHz to 1 Hz. The resulted impedance spectra were fit using Z-View software. The Nyquist plots and the best fit results (Figure S2 of the supplementary material)[13] based on an equivalent circuit were described in the supplementary material.

In Figure 1 one-step and two-step coating procedures are schematically illustrated. For one-step coating of $CH_3NH_3PbI_3$, the DMA solution containing equimolar CH_3NH_3I and PbI_2 is spin-coated on the mesoporous TiO_2 layer. PbI_2 is formed first for two-step coating procedure, which was followed by spin-coating the CH_3NH_3I solution. In two-step procedure, compared to two-step dipping method,[3] two-step spin-coating procedure is well defined method because of quantitatively managed process. The amount of CH_3NH_3I and spin-coating condition should be carefully adjusted in terms of the amount of deposited PbI_2. For coating with 20 μl of 1M PbI_2 solution, 100 μl of 0.063M CH_3NH_3I is found to be sufficient to convert PbI_2 into $CH_3NH_3PbI_3$ as confirmed by no presence of PbI_2 peak in X-ray diffraction spectrum (data are not shown). Detailed method for two-step coating is described in the experimental part.

As can be seen in SEM images in Figure 2, morphology of the deposited $CH_3NH_3PbI_3$ is remarkably different. One-step coating produces shapeless $CH_3NH_3PbI_3$ (Figure 2(b)), whereas cube-like crystals are formed by two-step coating method (Figure 2(c)). Besides morphological difference, TiO_2 layer is not completely covered by the perovskite using one-step spin-coating method compared to full coverage with perovskite by two-step coating procedure. Insufficient coverage in one-step coating is probably related to wettability, associated with high ionic strength (1.25M of $CH_3NH_3^+$ and Pb^{2+} and 3.75M of I^-) of coating solution,[14] and/or competition between positive ions of $CH_3NH_3^+$ and Pb^{2+}. Contrary to one-step method, close packing with cube-like

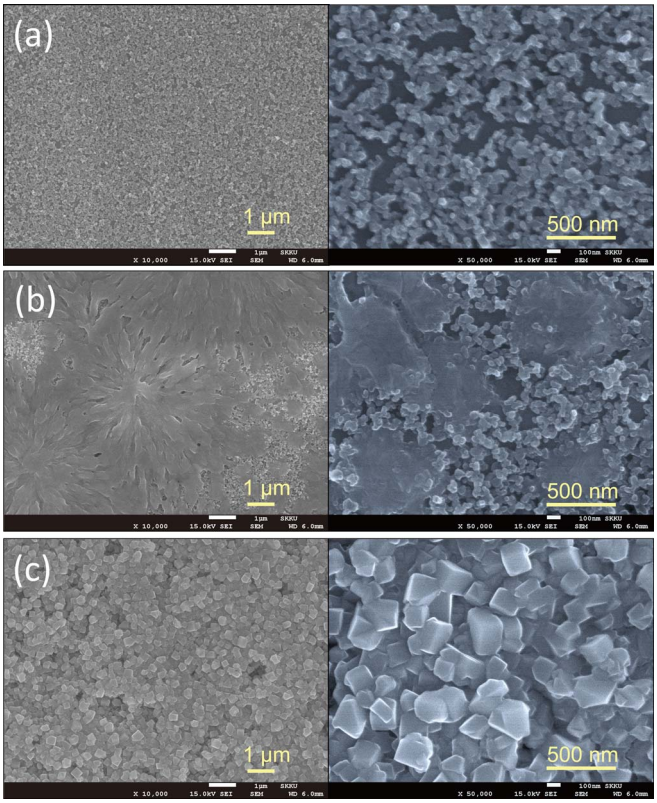

FIG. 2. Surface SEM images (left: low magnification, right: high magnification) of (a) mesoporous TiO_2 coating on the compact blocking layer deposited FTO substrate, (b) one-step deposition of $CH_3NH_3PbI_3$ on the mesoporous TiO_2 layer, and (c) two-step deposition of $CH_3NH_3PbI_3$ on the mesoporous TiO_2 layer.

crystal with dimension of about 100–150 nm is induced by two-step method, which indicates that spin-coating of 20 μl of 1M solution of PbI_2 in DMF covers fully the TiO_2 film. PbI_2 is layered structure and well known to undergo intercalation reaction,[15] in which Lewis base molecules such as pyridine and methylamine were found to be intercalated into interlayer of PbI_2. It was mentioned that charge transfer was not obvious during intercalation reaction and the dipole moment of Lewis base molecule or hydrogen bonding by the N–H bond was necessary requirement for intercalation. Thus, reaction of PbI_2 with CH_3NH_3I may be regarded as pseudo-intercalation because I^- in CH_3NH_3I salt acts as an electron donor. Reaction of PbI_2 with I^- forms presumably $(PbI_3)^-$ via I_2-I^- interaction, which is followed by reaction with $CH_3NH_3^+$ to form $CH_3NH_3PbI_3$. It was reported that a vacuum deposited PbI_2 was converted to $CH_3NH_3PbI_3$ when it was dipped in CH_3NH_3I solution, where full conversion required more than 1 h.[16] However, solution processed PbI_2 film reduces significantly reaction time for conversion. According to single crystal X-ray diffraction analysis, need-like crystals collected after cooling 1M solution of PbI_2 in DMF revealed that one DMF molecule was coordinated to Pb via oxygen bridge.[17] Thus, substitution of CH_3NH_3I for DMF could also explain the two-step formation of $CH_3NH_3PbI_3$[17] and the faster reaction than the vacuum deposited PbI_2 beginning with surface reaction.

Investigation from cross-sectional SEM images also confirms imperfect pore-filling of perovskite by one-step coating, which leads to contact between FTO and HTM as can be seen in Figure 3. On the other hand, pores are completely filled with perovskite by using two-step coating. As can be seen in schematic illustrations based on SEM images, one-step coating leads to perovskite island but two-step one results in void-free perovskite layer. Mesoporous TiO_2 layer thickness is about 100 nm and perovskite overlayer is around 200 nm.

Photovoltaic parameters are plotted in Figure 4, where the data obtained from 40 cells are statistically analyzed. All the parameters of two-step deposited perovskite are superior to those of

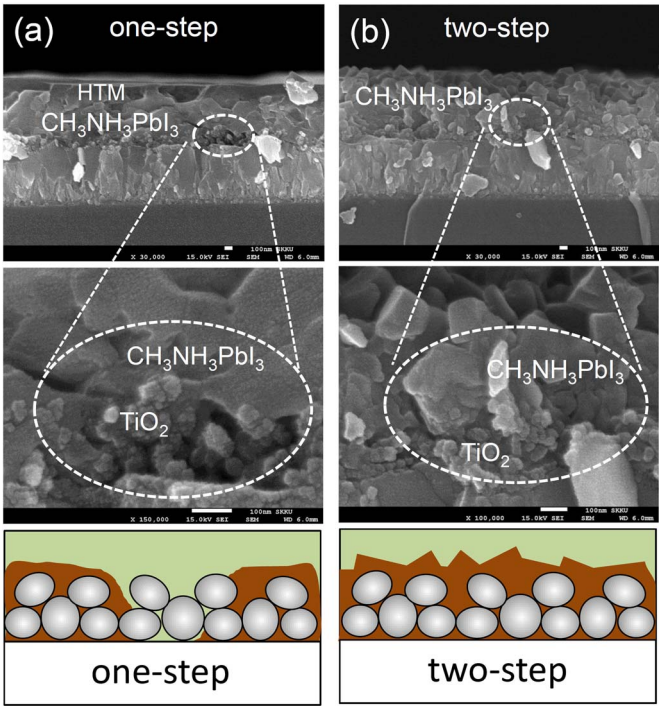

FIG. 3. Cross sectional SEM images of (a) one-step deposition of $CH_3NH_3PbI_3$ and (b) two-step deposition of $CH_3NH_3PbI_3$. One-step deposition leads to imperfect pore-filling as shown in the high magnification SEM image. Two-step deposition shows that pores of TiO_2 layer are fully filled with $CH_3NH_3PbI_3$ as confirmed by void-free interface.

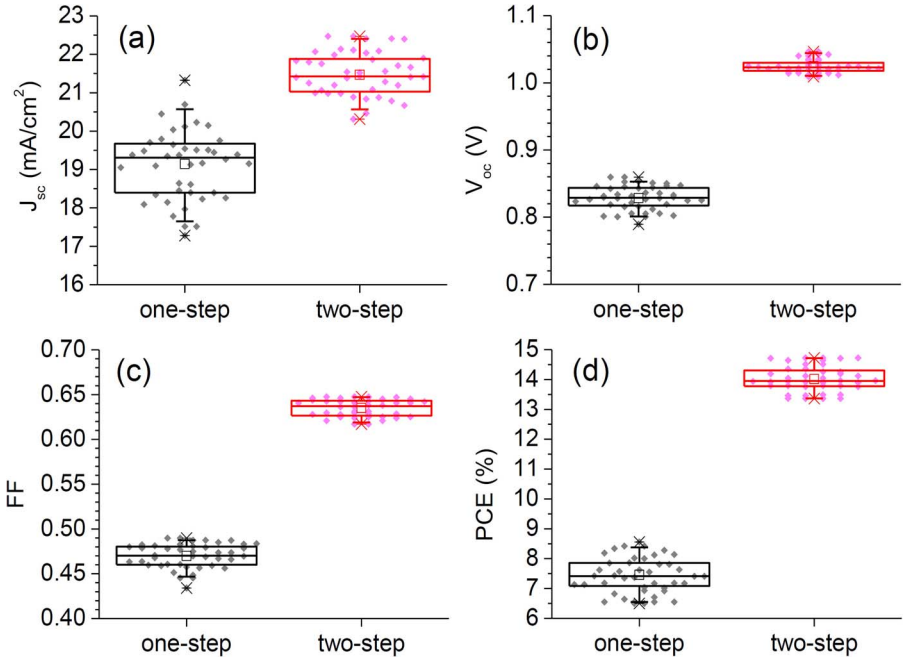

FIG. 4. Short-circuit current density (Jsc), open-circuit voltage (V_{oc}), fill factor (FF), and power conversion efficiency (PCE) for the perovskite solar cells based on one-step and two-step deposition procedure. The data were statistically analyzed from 40 cells.

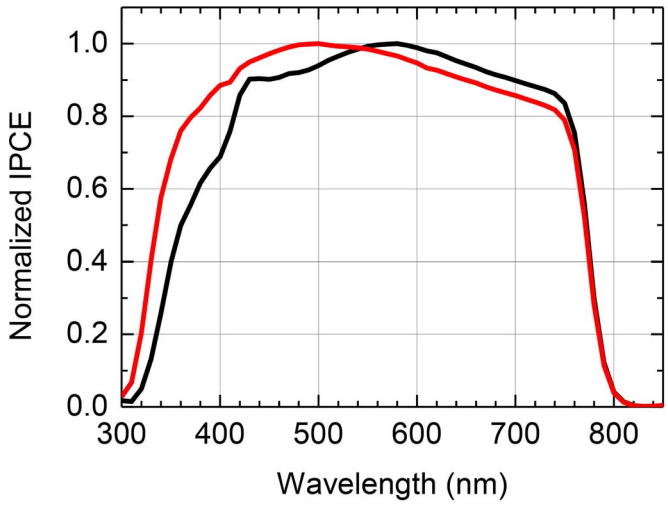

FIG. 5. Normalized IPCE for the perovskite solar cells based on one-step (black line) and two-step (red line) process.

one-step deposited one. Average short-circuit current density (J_{sc}), open-circuit voltage (V_{oc}), fill factor (FF), and power conversion efficiency (PCE) of 19.15 mA/cm^2, 0.828 V, 0.470, and 7.5% are observed from the one-step deposited perovskite solar cells, while higher values of 21.47 mA/cm^2, 1.024 V, 0.634, and 13.9% are obtained from the two-step deposited ones. Standard deviation for PCE is as small as ±0.6 and ±0.4 for the one-step and two-step deposited devices, respectively, which indicates that the data are reproducible. Morphology-property relation can explain difference in photovoltaic performance. Higher J_{sc} for the two-step deposition is due to better pore-filling of perovskite compared to its island structure for the one-step deposition. As shown in Figure 3, the absence of perovskite at FTO interface loses absorption of short wavelength light, as firmed by IPCE measurement in Figure 5, which is responsible for lower J_{sc} for one-step deposition.

Recombination kinetics of devices based on one-step and two-step procedure are investigated using a transient photovoltage measurement and impedance spectra. The electron life time is obtained from a transient photovoltage signal by fitting it with first order exponential decay. In the transient photovoltage measurement the electron life time is strongly dependent on the light intensity where strong light intensity induces high electron and hole density and thus, a fast recombination is resulted. Contrariwise, longer electron life time is attributed to the lower density of electron and hole induced by weak light intensity.[18] It is reported that $CH_3NH_3PbI_3$ perovskite solar cell also shows the power law dependence of electron life time on the light intensity or open circuit voltage,[19,20] as shown in Figure 6(a). The electron life time of two-step deposited perovskite is about one order of magnitude longer than that of one-step implying that the recombination kinetics highly depends on the perovskite structure determined by deposition method. This suggests that the voids generated in one-step coating allow HTM to infiltrate into perovskite layer, which increases a potential recombination site and leads ten times faster recombination than in two-step deposited perovskite. The recombination resistance is obtained from impedance spectra where the first arc in high frequency region is related to the transport in sprio-MeOTAD[21] and the second arc is related to the recombination.[22,23] The two arcs are fitted using a simplified equivalent circuit (resistance-parallel resistance, capacitance-parallel resistance, and capacitance in series) and the resulted recombination resistance (R_r) is plotted as a function of an applied bias voltage in Figure 6(b). R_r shows little change in the low applied voltage ($V_{app} < 0.5$ V) region but it starts to decrease rapidly as the Fermi level in photoanode increases by applying high bias voltage ($V_{app} > 0.5$ V).[1] R_r for one-step and two-step deposited perovskite are similar as expected in the region of low applied voltage ($V_{app} < 0.5$ V), but R_r for one-step shows lower value than that for two-step as the applied bias voltage increases more than 0.5 V describing that the recombination kinetics for one-step is faster than that of two-step perovskite. This result is also accordance with the tendency of electron life time. Likewise, the two-step perovskite shows enhanced recombination kinetics due to its well established layer with free-void

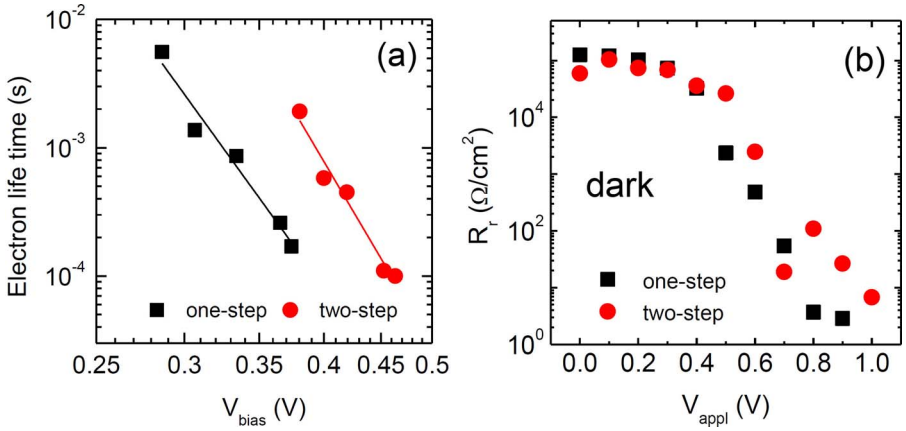

FIG. 6. Comparison of (a) electron life time for one-step (black) and two-step (red) deposited perovskite with varying open circuit voltage and (b) recombination resistance for one-step (black) and two-step (red) deposited perovskite by applying bias voltage.

enabling to prevent the HTM infiltration and thus decrease the recombination probability. The lowered recombination rate for two-step deposited perovskite layer has a significant impact on the open-circuit voltage[24] leading 200 mV higher V_{oc} than that for one-step deposited perovskite. It was reported that photovoltaic performance was found to be strongly dependent on degree of perovskite pore-filling, where decrease in perovskite pore-filling fraction led to deterioration of J_{sc}, V_{oc}, and fill factor.[25] In addition, incomplete perovskite pore-filling resulted in fast charge recombination of the injected electron in TiO_2 with spiro-MeOTAD.[25] Thus, we propose here that removal of the exposed TiO_2 allowing unwanted contact with spiro-MeOTAD is important to improve photovoltaic performance of the mesoporous TiO_2 based perovskite solar cell.

Photovoltaic property-morphology relation was systematically evaluated from the diverse deposition methodologies of perovskite $CH_3NH_3PbI_3$. Reproducible photovoltaic parameters extracted from statistical analysis were found to have strong correlation with the morphology of the deposited perovskite along with degree of the perovskite coverage. Recombination kinetics was significantly affected by the resulting morphology of the perovskite. The exposed TiO_2 by one-step coating was responsible for fast recombination and short electron life time. On the other hand, the complete pore-filling with perovskite by two-step method resulted in a significant improvement of photovoltaic performance. It is concluded that photovoltaic performance is strongly dependent on degree of perovskite coverage on the mesoporous TiO_2 layer and morphology of the deposited perovskite in the mesoporous TiO_2 based perovskite solar cells.

This work was supported by the National Research Foundation of Korea (NRF) grants funded by the Ministry of Science, ICT & Future Planning (MSIP) of Korea under Contract Nos. NRF-2010-0014992, NRF-2012M1A2A2671721, NRF-2012M3A7B4049986 (Nano Material Technology Development Program), and NRF-2012M3A6A7054861 (Global Frontier R&D Program on Center for Multiscale Energy System). H.S.K. is grateful to NRF for funding the global Ph.D. grant.

[1] H.-S. Kim, C.-R. Lee, J.-H. Im, K.-B. Lee, T. Moehl, A. Marchioro, S.-J. Moon, R. Humphry-Baker, J.-H. Yum, J. E. Moser, M. Grätzel, and N.-G. Park, Sci. Rep. **2**, 591 (2012).
[2] M. M. Lee, J. Teuscher, T. Miyasaka, T. N. Murakami, and H. J. Snaith, Science **338**, 643 (2012).
[3] J. Burschka, N. Pellet, S.-J. Moon, R. Humphry-Baker, P. Gao, M. K. Nazeeruddin, and M. Grätzel, Nature (London) **499**, 316 (2013).
[4] M. Liu, M. B. Johnston, and H. J. Snaith, Nature (London) **501**, 395 (2013).
[5] A. Kojima, K. Teshima, Y. Shirai, and T. Miyasaka, J. Am. Chem. Soc. **131**, 6050 (2009).
[6] J.-H. Im, C.-R. Lee, J.-W. Lee, S.-W. Park, and N.-G. Park, Nanoscale **3**, 4088 (2011).
[7] J. H. Heo, S. H. Im, J. H. Noh, T. N. Mandal, C.-S. Lim, J. A. Chang, Y. H. Lee, H.-j. Kim, A. Sarkar, M. K. Nazeeruddin, M. Grätzel, and S. I. Seok, Nat. Photon. **7**, 486 (2013).
[8] N.-G. Park, J. Phys. Chem. Lett. **4**, 2423 (2013).
[9] H. J. Snaith, J. Phys. Chem. Lett. **4**, 3623 (2013).

[10] H.-S. Kim, S. H. Im, and N.-G. Park, J. Phys. Chem. C **118**, 5615 (2014).
[11] S. Kazim, M. K. Nazeeruddin, M. Grätzel, and S. Ahmad, Angew. Chem. Inter. Ed. **53**, 2812 (2014).
[12] P. P. Boix, K. Nonomura, N. Mathews, and S. G. Mhaisalkar, Mater. Today **17**, 16 (2014).
[13] See supplementary material at http://dx.doi.org/10.1063/1.4891275 for the real device configuration and for the Nyquist plots and their fits based on an equivalent circuit.
[14] R. Steitz, W. Jaeger, and R. V. Klitzing, Langmuir **17**, 4471 (2001).
[15] C. C. Coleman, H. Goldwhite, and W. Tikkanen, Chem. Mater. **10**, 2794 (1998).
[16] K. Liang, D. B. Mitzi, and M. T. Prikas, Chem. Mater. **10**, 403 (1998).
[17] A. Wakamiya, M. Endo, T. Sasamori, N. Tokitoh, Y. Ogomi, S. Hayase, and Y. Murata, Chem. Lett. **43**, 711–713 (2014).
[18] K. Zhu, S.-R Jang, and A. J. Frank, J. Phys. Chem. Lett. **2**, 1070 (2011).
[19] D. Bi, S.-J. Moon, L. Haggman, G. Boschloo, L. Yang, E. M. J. Johansson, M. K. Nazeeruddin, M. Grätzel, and A. Hagfeldt, RCS Adv. **3**, 18762 (2013).
[20] Y. Zhao, A. M. Nardes, and K. Zhu, J. Phys. Chem. Lett. **5**, 490 (2014).
[21] F. Fabregat-Santiago, J. Bisquert, L. Cevey, P. Chen, M. Wang, S. M. Zakeeruddin, and M. Grätzel, J. Am. Chem. Soc. **131**, 558 (2009).
[22] H.-S. Kim, I. Mora-Sero, V. Gonzalez-Pedro, F. Fabregat-Santiago, E. J. Juarez-Perez, N.-G. Park, and J. Bisquert, Nat. Commun. **4**, 2242 (2013).
[23] H.-S. Kim, J.-W. Lee, N. Yantara, P. P. Boix, S. A. Kulkarni, S. Mhaisalkar, M. Grätzel, and N.-G. Park, Nano Lett. **13**, 2412 (2013).
[24] A. Zaban, M. Greenshtein, and J. Bisquert, Chem. Phys. Chem. **4**, 859 (2003).
[25] T. Leijtens, B. Lauber, G. E. Eperon, S. D. Stranks, and H. J. Snaith, J. Phys. Chem. Lett. **5**, 1096 (2014).